Adv Syst Sci Appl 2018; **1**; 59-84
Published online at http://ijassa.ipu.ru.

Analytical study of the antitumor viral vaccine introduction regimens based on mathematical modeling

Nina A. Babushkina[1], Ekaterina A. Kuzina[1]

[1)] *V.A. Trapeznikov Institute of Control Sciences of Russian Academy of Sciences, 117997, Profsoyuznaya street, 65, Moscow, Russia*

E-mail: babushkina_na@mail.ru, kate_k93@mail.ru

Abstract. The paper presents the algorithm for calculating the maximal effective antitumor viral vaccine introduction regimens, using a computing experiment method (in silico) based on the software implementation of two mathematical models in the MatLab-Simulink system. The first model of antitumor vaccine therapy describes a two-stage mechanism of the tumor cells' death as a result of the immune response. The effectiveness of immune response is measured in the number of antibodies formed by the immune system against virus-infected tumor cells. The second model of antitumor therapy with discontinuous trajectories of tumor growth is designed to evaluate the rate of the tumor cells' death after the introduction of the viral vaccine. The effectiveness of the therapy is measured in the number of dying tumor cells after the introduction of a viral vaccine.

Keywords: mathematical model, experimental oncology, tumor cells, kinetic curves of tumor growth, tumor growth delay, virus, vaccine therapy, immune response, number of antibodies, vaccine efficacy, time-frame for recurrent vaccine introductions, in silico.

1. INTRODUCTION

Vaccine therapy is one of the methods of immune therapy of the oncological diseases. It implies vaccination against the malignant cells formed in the body. As with any vaccination, the introduction of viral vaccines stimulates the body's immune system and causes the formation of antibodies specific to the tumor type. Experiments in tumor immunotherapy can be traced back to Ehrlich [1], and since the middle of the twentieth century the studies aiming to find the viruses that are able to affect malignant tumors without causing any harm to the humans commenced in the Soviet Union and were further continued in Russia [2-6].

One of approaches to developing effective antitumor vaccines implies using the viruses that are able to identify malignant cells and do not cause any damage to the normal tissues. The viruses selected for therapy should be clinically harmless and epidemiologically safe. Therefore, oncotropic viruses must have a genetically fixed absence of pathogenic properties and be unable to cause an acute infectious disease in a human body.

Among the viruses that meet these criteria are the Venezuelan horse encephalomyelitis virus (VEE) [5-7] and rat parvovirus H-1 [15-23]. Both are not harmful to humans because they do not affect healthy tissues since they cannot replicate in the non-dividing cells [16-18]. Thus these viruses are able to identify the tumor cells based on their high proliferation rates, and specifically target them without attacking the normal tissues [18-19].

Experimental studies of rat parvovirus H-1 indicate that there are two possible mechanisms of the tumor cells' death as a result of vaccine introduction. Firstly, the virus blocks the cycle of the tumor cells [16-18]. Secondly, it produces specific protein formations on the tumor cell surface that stimulate the immune system to develop antibodies against these cells, resulting in their death [13-14, 19-21]. This corresponds to the results of the experimental studies of the impact of the VEE virus on tumor growth [4-6]. However, since such experiments require

extensive funding, these studies did not determine the maximal and minimal effective dosages and the optimal moment of vaccine introduction.

Thus, the present study presents an algorithm that allows to determine the optimal dosage of the VEE virus-derived vaccine and the moment of its introduction that will ensure the maximal rate of tumor cells' death, building on the mathematical models of anti-tumor therapy and vaccine therapy developed in [7-9].

2. THE MATHEMATICAL MODEL OF THE VEE VIRUS VACCINE THERAPY

The mathematical model of vaccine therapy describes the mechanism of two-stage death of tumor cells caused by the virus itself and as a result of the immune system stimulation against the infected tumor cells.

Based on the experimental data on the growth of Erlich adenocarcinoma in mice after a single introduction of the VEE virus vaccine, one day after the tumor was transplanted to animals (Figure 1), the parameters of the model were estimated and its adequacy was tested using experimental dosages of the VEE virus vaccine [8-11]. The values of the model parameters are shown in Appendix 1.

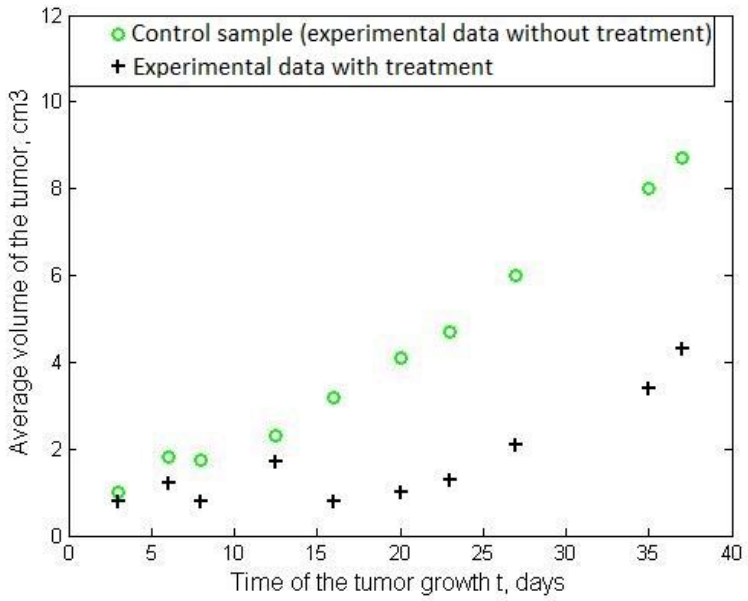

Fig. 1. Experimental curves of the Ehrlich adenocarcinoma growth without vaccine administration (control) and after single vaccine administration

The mathematical model of the two-stage death of tumor cells after the viral vaccine introduction is described by the following system of differential equations (1-8) [7-10]:

$$\frac{dN_V(t)}{dt} = \lambda(t)\cdot N(t)\cdot\theta(t_V - t) + \left[\lambda\left(t-t_V\right) - K_V V(t-t_V) - K_{AV}A_V\left(t-t_V\right)\right]\cdot N_V\left(t-t_V\right)\theta(t_N - t) + \\ + \left[\lambda\left(t-t_N\right) - K_{AN}A_N\left(t-t_N\right)\right]\cdot N(t-t_N) \quad (1)$$

where $V(t)$ is the number of viruses, $N(t)$ is the number of tumor cells without vaccine introduction, described by the following differential equation:

$$\frac{dN(t)}{dt} = \lambda(t)\cdot N(t)\text{, at } N(t_0) = N_0 \quad (2)$$

where λ(t) is the rate of tumor cells' proliferation,

$N_V(t)$ is the number of infected tumor cells after the vaccine introduction,

$t_V = \tau_1 + Z_{CV}$ is the moment of the start of immune response against viruses,

$t_N = \tau_1 + Z_{CN}$ is the moment of the start of immune response against tumor cells,

τ_1 is the moment of vaccine introduction,

Z_{CV} and Z_{CN} are the time lag of immune response against the virus and infected tumor cells,

$A_V(t - t_V)$ is the number of antibodies against the virus,

$A_N(t - t_N)$ is the number of antibodies against infected tumor cells,

$\theta(t_V - t)$ and $\theta(t_N - t)$ are the Heaviside step function,

K_{AV}, K_{AN}, and K_V are the dimension factors.

The first component of equation (1) describes the dynamics of the tumor cells' growth before the introduction of the viral vaccine.

The second component of equation (1) describes the death of infected tumor cells caused by the virus.

The first stage of the immune system stimulation is production of antibodies against the virus (Figure 2 – $C_V(t)$, $A_V(t)$). At this stage the death of tumor cells is caused by the penetration of the virus inside the tumor cells (Figure 3).

The third component of the equation describes the death of tumor cells caused by antibodies produced against the infected tumor cells (Figure 2 – $C_N(t)$, $A_N(t)$). Reproducing in tumor cells, the viruses induce the development of new protein formations on the surface of the tumor cell membranes. Such infected tumor cells are perceived by the immune system as foreign to the body. As a result, immune system produces antibodies specific to the tumor cells, and they destroy the infected tumor cells (Figure 3).

The patterns of immune response to the foreign cells are based on Marchuk's mathematical model of infectious diseases [24-27]. This model treats the immune response (production of T and B cells) as a combined action. Therefore in the present study the immune response means the formation of antibodies and plasma cells specific to the VEE virus and infected tumor cells.

Using Marchuk's model, the dynamics of the number of viruses is described by the following equation:

$$\frac{dV(t)}{dt} = \alpha_V V(t) - \beta_V A_V(t) V(t), \tag{3}$$

where $V_0 = V(\tau_1)$ is the initial dose of the viral vaccine, τ_1 is the moment of the first administration of the viral vaccine, α_V is the rate of viruses' reproduction within the cell,

β_V is the death rate of viruses when they interact with antibodies $A_V(t)$.

In the vaccine therapy model, the initial condition $V_0 = V(\tau_1)$ denotes the dosage of the vaccine. The immune response of the body to the virus introduction results in production of antibodies and plasma cells. Their numbers are calculated using the following four differential equations [24-25] for each of the two stages of the immune response – against the virus and against the infected tumor cells.

The dynamics of the number of antibodies to the virus $A_V(t)$:

$$\frac{dA_V(t)}{dt} = \alpha_A C_V(t - t_V) - \beta_{AV} A_V(t - t_V) V(t - t_V) - \beta_V A_V(t - \tau_1), \tag{4}$$

where α_A is the rate of formation of antibodies from a single plasma cell, β_{AV} is the death rate of antibodies due to interaction with viruses $A_V(t)$, β_V is the rate of decrease in the number of antibodies due to natural destruction.

The dynamics of formation of plasma cells $C_V(t)$:

$$\frac{dC_V(t)}{dt} = \alpha_C V(t-\tau_1) A_V(t-t_V) - \beta_{CV}\left[C_V(t-\tau_1) - C_{VN}\right], \text{ at } C_V(\tau_1) = C_{VN}, \quad (5)$$

where α_C is the rate of formation of plasma cells, β_{CV} is the dimension factor, Z_{CV} is the time lag of the immune response to the formation of a plasma cell clone. The second term of this equation defines the deviation of the actual number of plasma cells from the norm C_{VN}.

The equation for the dynamics of the number of antibodies $A_N(t)$ acting against infected tumor cells is as follows:

$$\frac{dA_N(t)}{dt} = \alpha_{AN} C_N(t-t_N) - \beta_{AN} A_N(t-t_N) N_V(t-t_N) - \beta_{NN} A_N(t-t_N), \quad (6)$$

where α_{AN} is the rate of formation of antibodies from a single plasma cell, β_{AN} is the death rate of antibodies $A_N(t)$ due to interaction with infected tumor cells $N_V(t)$, β_{NN} is rate of decrease in the number of antibodies due to natural destruction.

The dynamics of formation of plasma cells $C_N(t)$:

$$\frac{dC_N(t)}{dt} = \alpha_{CN} N_V(t) A_N(t-t_N) - \beta_{CN}\left[C_N(t-t_N) - C_{NN}\right], \quad (7)$$

at $C_{AN}(\tau_1) = C_{NN}$, where α_{CN} is rate of formation of plasma cells, β_{CN} is the dimension factor, Z_{CN} is the time lag of the immune response to the formation of a plasma cell clone against the infected tumor cells.

Dynamics of antibodies $A_V(t)$ against the virus and against infected tumor cells $A_N(t)$ are shown in Figure 2.

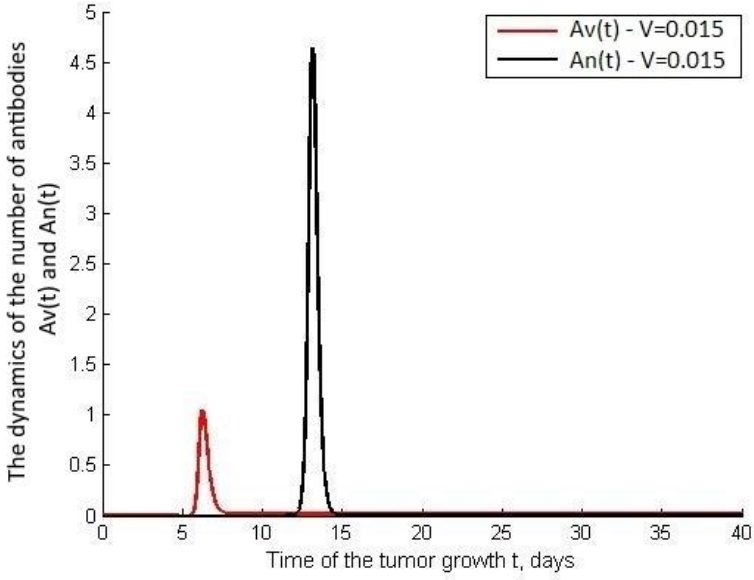

Fig. 2. Population dynamics of antibodies $A_V(t)$ against the virus and against infected tumor cells $A_N(t)$ for experimental dosage $V_0 = 0,015$ on τ_1 = day 1 (the first and second stages of the immune response)

In the equations that describe the dynamics of the formation of antibodies (6) and plasma cells (7), the number of infected tumor cells was calculated as $N_V(t) = N(t_N) \cdot P(t_N)$, where $P(t_N)$ accounts for the proportion of rapidly proliferating cell fraction as the size of the tumor increases [14]:

$$P(t) = 1 - \left[\frac{1}{\pi K_p} arctg\left(\frac{2\alpha_p \beta_p \cdot t}{1 - \beta_p^2 \cdot t^2}\right) \right], \quad (8)$$

where α_p *and* K_p are constant parameters, t is the current time of the tumor cell population growth, $\beta_p = \frac{1}{t^*}$, where t^* is the moment when the numbers of the rapidly and slowly proliferating cells are equal.

The fraction of rapidly proliferating tumor cells is located near the blood vessels (oxygenated fraction), while the fraction of slowly proliferating cells is pushed to the tumor periphery (hypoxic fraction). The process of the change in the proportion of the rapidly and slowly proliferating cells with the increase in the tumor size is described in the Skipper model [31]. As the number of the fast-proliferating tumor cells decreases, the virus ceases to affect them. This causes the decrease of the tumor sensitivity to the viral vaccines and of the number of infected tumor cells $N_V(t)$ that can induce the immune response. As a result, the number of the antibodies developed against tumor cells is reduced, and the effectiveness of the viral vaccines declines.

Thus, the mathematical model of vaccine therapy describes the mechanism of two-stage death of tumor cells caused by the virus itself and as a result of the immune system stimulation against the infected tumor cells.

The calculated curves that describe the dynamics of the two-stage death of infected tumor cells $N_V(t)$ and the production of antibodies and plasma cells at the each of the two stages of the immune system stimulation are shown in Figure 3 [8-10].

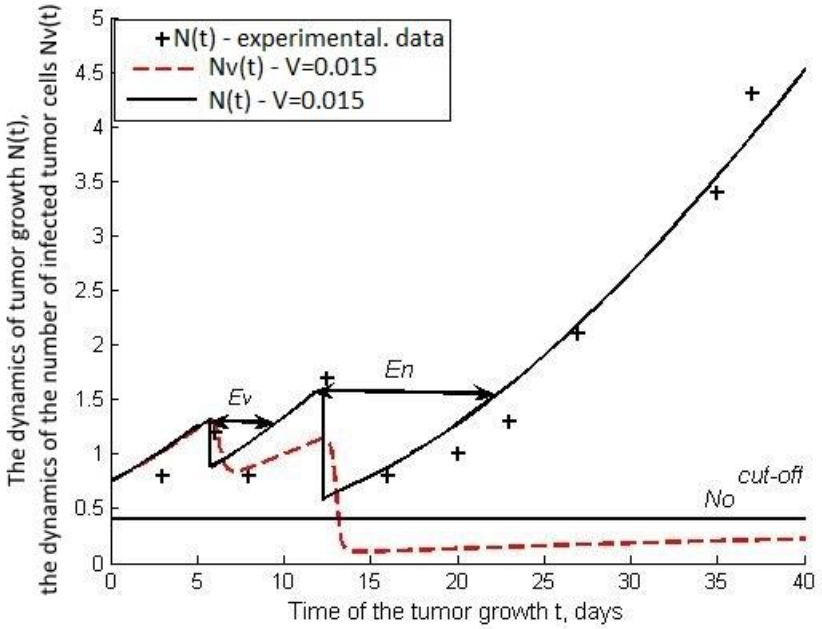

Fig. 3. Calculated growth curve of the total number of tumor cells $N(t)$ (full line) that approximates experimental data (+) based on the mathematical model of antitumor therapy (dosage $V_0 = 0,015$ on τ_1 = day 1); the dotted line indicates the dynamics of the number of infected tumor cells $N_V(t)$.

Calculations show that the curve that describes the dynamics of the number of infected tumor cells is located below the experimental curve of the tumor growth. This indicates that when the viral vaccine is administered, it does not infect the entire tumor cell population $N(t)$. Some cells remain uninfected $N_R(t)$ and continue to multiply, causing a repeated growth of the tumor, as observed in the experiment (Figure 1). Some cells survive (RN_0^V – after the 1st stage of immune response, RN_0^N – after the 2nd stage), causing a repeated growth of the tumor as observed in the experiment (Figure 1).

3. THE MATHEMATICAL MODEL OF ANTITUMOR THERAPY WITH DISCONTINOUS TRAJECTORIES FOR ASSESSING THE TUMOR GROWTH DELAY AFTER THE TWO-STAGE DEATH OF TUMOR CELLS

The mathematical model of antitumor therapy with discontinuous trajectories was developed to control and optimize the regimes of applying different antitumor therapy methods based on kinetic curves of tumor growth [8-10].

Figure 3 shows the calculated growth curve of the total number of tumor cells $N(t)$ (full line), which was obtained based on the mathematical model of antitumor therapy by approximating the experimental data.

The duration of tumor growth delay was estimated based on the following assumptions adopted in the mathematical model of antitumor therapy [8-10]:

1. The cell death occurs instantly at each of the two stages of the immune system stimulation. The abrupt decrease in the tumor size occurs at the moment when the maximal number of antibodies to the virus and infected tumor cells is produced.

2. Reduction in the tumor size occurs only due to the death of the virus-infected tumor cells.

3. The surviving tumor cells continue to grow at the same reproduction rate. The kinetic curves of their growth are described by the Gompertz function, keeping the parameters of the tumor growth without treatment (control), but accounting for the time shift caused by tumor growth delay $\varepsilon_V(V_0)$ and $\varepsilon_N(V_0)$ after each stage of their death (Figure 4).

According to the basic antitumor therapy model [8-10], the kinetic curves of tumor growth without treatment are described by a simple differential equation

$$\frac{dN(t)}{dt} = \alpha_N \beta_N \exp(-\beta_N t) N(t), \; at \; N(0) = N_0, \tag{9}$$

where N_0 is the initial number of tumor cells at the time of tumor transplantation to animals at $t = 0$, $N(t)$ is the number of cells in the tumor at time t, α_N and β_N are the parameters of the Gompertz function, which approximates the experimental kinetic curve of Ehrlich adenocarcinoma growth without treatment (Figure 1) [5-7, 10-14].

Based on the assumptions listed above, tumor growth after the introduction of viral vaccines follows a differential equation describing the two-stage death of tumor cells:

$$\begin{aligned}\frac{dN(t)}{dt} = {} & \lambda(t)N(t)\theta(t_V - t) - S_V(V_0, \tau_1)N(t_V)\delta(t - t_V) + \lambda(t - t_V)N(t - \varepsilon_V(V_0))\theta(t_N - t) - \\ & - S_N(N_V, \tau_1)N(t_N)\delta(t - t_N) + \lambda(t - t_N)N(t - \varepsilon_N(V_0)),\end{aligned} \tag{10}$$

where $N(t)$ is the total number of tumor cells at time t,

$\lambda(t)$ is the growth rate of a given type of a tumor,

$\theta(t_V - t)$ and $\theta(t_N - t)$ is the Heaviside step function,

$t_V = \tau_1 + Z_{CV}$ and $t_N = \tau_1 + Z_{CN}$ are the moments of the tumor cells' death at each of the two stages of the immune system stimulation,

τ_1 is the moment of the viral vaccine introduction,

Z_{CV} and Z_{CN} denote the time lag of the immune response against the virus and infected tumor cells,

$\delta(t-t_V)$ and $\delta(t-t_N)$ are the Dirac delta function describing instant death of tumor cells at each of two stages of the immune system stimulation,

$S_V(V_0,t_V)$ and $S_V(V_0,t_N)$ are the relative decrease in the tumor size at the time the tumor cells' death at each of the two stages,

$\varepsilon_V(V_0,t_V)$ and $\varepsilon_N(V_0,t_N)$ are the tumor growth delay after cells' death at each of the two stages of the immune system stimulation (Figure 3).

In the vaccine therapy model, it was assumed that the relative decrease in tumor volume occurs only due to the death of the virus-infected tumor cells $N_V(t)$. Thus in this model the number of dying cells was calculated as the difference between the maximum and minimum number of infected cells:

$$\Delta N_V(t_V) = Nv(t_1^V) - Nv(t_2^V) \quad \text{and} \quad \Delta N_V(t_N) = Nv(t_1^N) - Nv(t_2^N), \tag{11}$$

where t_1^V and t_1^N are the starting moments for the immune response against the virus and against the infected tumor cells,

t_2^V and t_2^N are the ending moments of the immune response.

According to the model of antitumor therapy, the relative decrease in tumor size at the time of the tumor cells' death at each of the two stages was determined from the following equations:

$$S_V(V_0,t_V) = \frac{\Delta N_V(t_V)}{N(t_V)} \quad \text{и} \quad S_N(V_0,t_N) = \frac{\Delta N_V(t_N)}{N(t_N)}, \tag{12}$$

where $N(t_V)$ and $N(t_N)$ denote the total number of cells in the tumor at the time points t_V and t_N.

The death of tumor cells causes tumor growth delay, and its duration serves as a quantitative measure of the cells' death depending on the dosage of the viral vaccine. The tumor growth delay $\varepsilon_V(V_0,t_V)$ and $\varepsilon_N(V_0,t_N)$ equals the time interval between the cells' death and their subsequent recovery to the original size at the moment of vaccine introduction (Figure 3):

$$N(t_V) = N(t_V + \varepsilon_V(V_0,t_V)) \quad \text{и} \quad N(t_N) = N(t_N + \varepsilon_N(V_0,t_N)). \tag{13}$$

Then the tumor growth after each stage of the infected cells' death is described by Gompertz equations with a time shift that accounts for the duration of the tumor growth delay as follows:

$$N(t-t_V) = RN_0^V \exp(\alpha_N(1-\exp(-\beta_N(t_V - \varepsilon_V(V_0))))), \tag{14}$$

$$N(t-t_N) = RN_0^N \exp(\alpha_N(1-\exp(-\beta_N(t_N - \varepsilon_N(V_0))))) \tag{15}$$

where RN_0^V and RN_0^N is the number of surviving cells after the 1st and the 2nd stages of immune response.

Figure 3 shows the calculated curve that describes the total number of tumor cells $N(t)$ (upper curve) derived from the mathematical model of antitumor therapy with discontinuous trajectories of tumor growth by approximating the experimental data. This curve describes the tumor growth $N(t)$ following three Gompertz equations (one for a control group) with a time shift that accounts for the tumor growth delay after each stage of the cells' death [8-10]. Appendix 1 shows the values of the parameters for the vaccine therapy model and the antitumor therapy model, estimated based on the experimental data provided in [10-14].

4. ALGORITHM FOR CALCULATING EFFECTIVE ADMINISTRATION REGIMENS FOR VIRAL VACCINES

Mathematical model of vaccine therapy and mathematical model of antitumor therapy with discontinuous trajectories of tumor growth were developed in MatLab-Simulink to conduct a computing experiment (in silico). The experiment aimed to identify the efficient vaccine therapy regimes for a wide range of VEE virus dosages and for different moments of vaccine introduction.

The efficiency of the vaccine therapy was assessed after each of the two stages of immune response based on two parameters:

1 – number of produced antibodies $A_V(t)$ and $A_N(t)$,

2 – number of dying tumor cells $\Delta N_V(t_V)$ and $\Delta N_V(t_N)$.

The efficiency of vaccine therapy method was estimated by two criteria. The first was the number of antibodies formed by the immune system at each of the two stages of its stimulation. We needed to determine the dosage that results in the maximum number of antibodies against infected tumor cells [10-13]. When this condition is met, the tumor-bearing organism is able to restrain the growth of the surviving tumor cells.

The second criterion was the tumor growth delay. It depends on the number of dying cells on each of the two stages of immune response.

Therefore, the algorithm for calculating optimal regimen of the viral vaccine is based on defining a maximal effective dosage when the immune system produces the biggest number of antibodies.

4.1. Calculating the viral vaccine dosage using the criterion of the production of antibodies against infected tumor cells

Based on the model of vaccine therapy with a single introduction of the varying dosages of the viral vaccines at the varying moments (from the 1st to 35th day), the graphs that show the changes in the number of antibodies against the virus $A_V(t)$ (Figure 4) and antibodies against infected tumor cells $A_N(t)$ (Figure 5) were developed [14].

These graphs reflect two fundamentally different types of the production of antibodies against the virus and against the tumor cells, depending on the vaccine dosage. The number of antibodies against the virus increases in proportion to the dosage increase, i.e. there is a linear dependence between these variables (Figure 4). However, the increase in the number of antibodies against infected tumor cells $A_N(V_0, \tau_1)$ is non-linear, and depends on the tumor size at the moment of vaccine introduction (Figure 5). This non-linear dependence allows determining the virus dose $V_0^{\max} = 0{,}024$ that results in the maximal production of antibodies against the infected tumor cells.

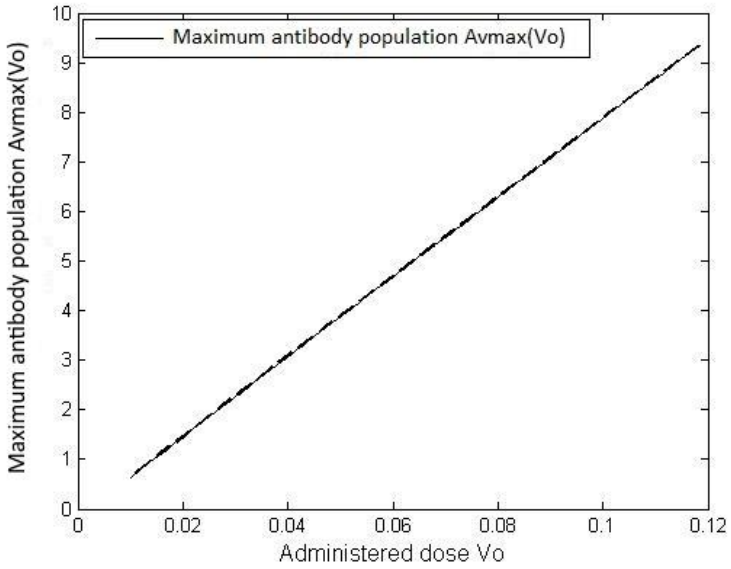

Fig. 4. Maximum number of antibodies against the virus $A_V^{\max}(V_0)$ depending on the dose V_0 administered on day 1 (the first stage of the immune system stimulation)

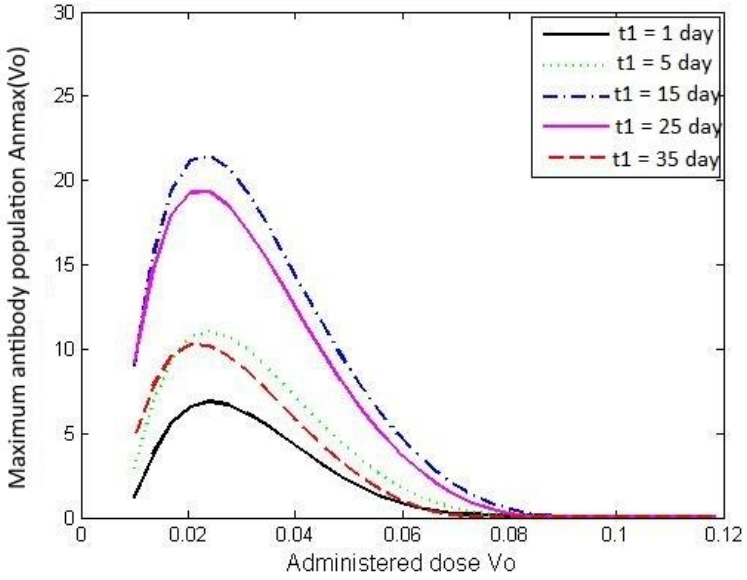

Fig. 5. Maximum number of antibodies against infected tumor cells $A_N^{\max}(V_0)$ depending on the dose of V_0 administered at different moments (the second stage of the immune system stimulation); τ_1 = 1, 5, 15, 25, 35 days

The non-linear dependence of production of antibodies on the dosage increase $A_N(V_0, \tau_1)$ may be due to the changes in the number of infected tumor cells on the 1st and 2nd stages of immune response. When the dosage is small, the number of the dying cells is low, but many cells get infected by the virus. With the further increase of the dosage exceeding $V_0^{\max}$ = 0,024, the number of cells dying at the 1st stage of immune response increases. This leads to reduction of the number of infected cells, and the consequent decrease in the number of antibodies against these cells on the 2nd stage of immune response.

Thus, with the administration of significant doses of the virus, almost the entire population of tumor cells is killed already at the 1st stage of immune response. This leads to a rapid and effective destruction of the tumor, but doesn't stimulate the 2nd stage of immune response; therefore the antibodies against the infected tumor cells are not produced.

The effectiveness of production of the antibodies against the infected tumor cells depends on the tumor size. As indicated by the calculations [14], after 35 days the number of fast-proliferating tumor cells starts to decrease, and this leads to the decline in the number of infected tumor cells and antibodies against them at the later stages of vaccine therapy.

Thus, the calculations using the mathematical model of vaccine therapy allowed to define the maximal effective dosage of the VEE virus-derived vaccine and to identify the moment of its administration that results in the maximal number of infected tumor cells $t^{\max}$ [14].

Based on the model of vaccine therapy the graphs that show the number of infected tumor cells that die at the 1st and 2nd stages of immune response were developed based on equation (11) (Figures 6 and 7).

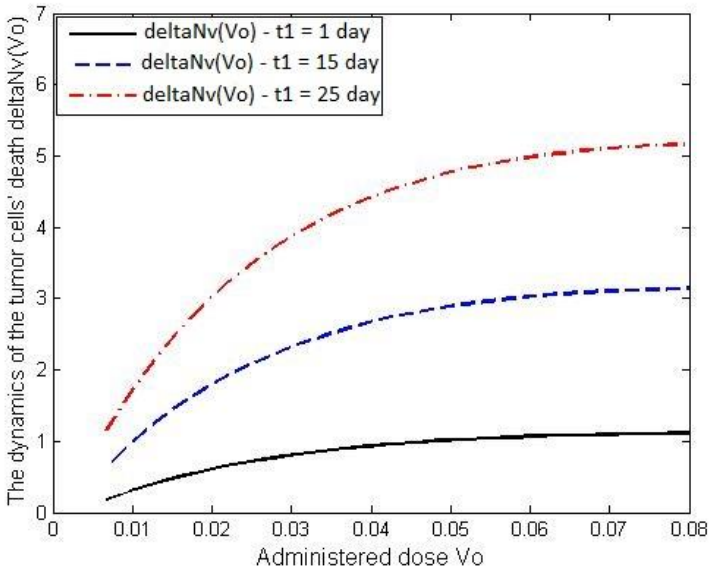

Fig. 6. Calculated curves describing the dynamics of the tumor cells' death $\Delta N_V^V(V_0)$ depending on the dosage on τ_1 = day 1, 15, 25 (1st stage of immune response)

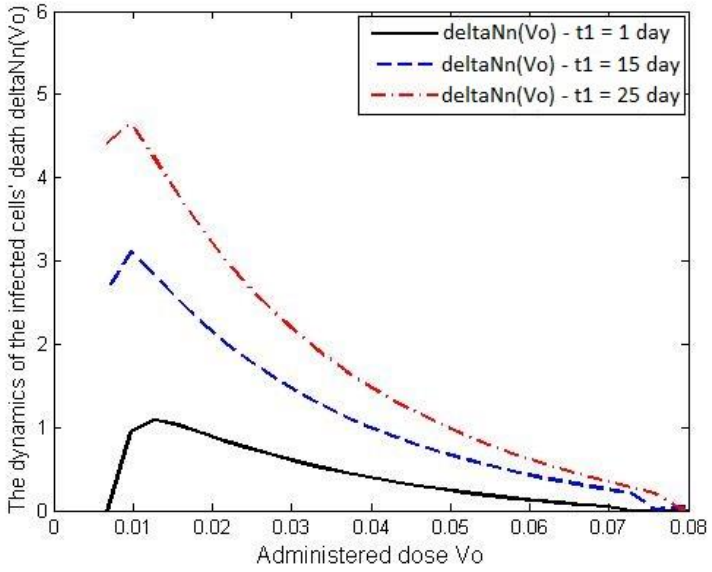

Fig. 7. Calculated curves describing the dynamics of the infected cells' death $\Delta N_V^N(V_0)$ depending on the dosage on τ_1 = day 1, 15, 25 (2nd stage of immune response)

There are fundamental differences in the dynamics of the tumor cells' death on each stage of the immune response. On the 1st stage the number of dying cells increases with the increase in the dosage, and depends on the tumor size at the moment of vaccine introduction (Figure 6). On the 2nd stage the number of dying cells declines due to the decreasing number of produced antibodies, as shown by the $A_N(V_0, \tau_1)$ graphs (Figures 5 and 7).

4.2. Kinetic curves of tumor cells' growth after 1st and 2nd stages of immune response

A model of antitumor therapy with discontinuous trajectories (Equations (9)-(16)) was used to forecast the dynamics of the tumor growth after the introduction of the viral vaccines in different regimes. Calculated curves of tumor growth are shown in Appendix 2.

The model includes a threshold value $N_0^{cut-off}$ that indicates the minimal number of the tumor cells that can trigger the renewed experimental tumor growth. After each of the two stages of tumor cells' death the tumor can resume its growth if the number of surviving cells RN_0^V and RN_0^N exceeds the threshold $N_0^{cut-off}$. Threshold value depends on the normal level of plasma cells C_{VN} and C_{NN} (Equations (5) and (7)). Threshold value was defined based on proportion $N_0^{cut-off} = \frac{N_0}{2} = \frac{0,76}{2} = 0,4$, where N_0 is the initial number of tumor cells (Equation (2)). If the number of surviving cells is below the threshold, then the tumor will not be able to resume its growth. In the model this is taken as complete elimination of tumor cells. In this case the lifetime of the vaccine-treated animals will be equal to the average lifetime of the experimental animals without treatment.

The resulting kinetic curves that describe tumor growth after vaccine introduction on $\tau_1 = 1$ day (Figures 8-15) allow to identify two dosage ranges that determine two possible regimens for administering antitumor vaccines.

The first regimen (with dosages exceeding $V_0 = 3 \cdot V_0^{\exp} = 0,045$) makes it possible to ensure that at the 1st stage of immune response the number of tumor cells drops below the threshold $N_0^{cut-off}$ (Figures 8-15), which is equivalent to elimination of tumor cells.

The second regime (with dosages between $V_0^{\exp} = 0,015$ and $3 \cdot V_0^{\exp} = 0,045$) does not produce the decline in the number of tumor cells below the threshold level $N_0^{cut-off}$. However, these dosages cause the death of the tumor cells at both stages of immune response, and this initiates the production of antibodies against infected cells. When these antibodies exist, the process of tumor growth can be controlled through recurrent introductions of the viral vaccine. This regimen will stabilize the initial tumor size. If the initial tumor size is small, this regimen makes it possible to avoid the surgical intervention, with vaccine therapy acting as a regular vaccination against autologous tumor cells.

The calculations show that if the vaccine is introduced on τ_1=25 day (Appendix 2) with dosages between $V_0^{\exp} = 0,015$ to $V_0 = 0,1$, the decrease of the number of tumor cells below the threshold level is not possible. Therefore if the tumor size is big, it needs to be surgically removed. However, if the surgical intervention is contraindicated, the tumor size can be stabilized through recurrent vaccinations. In any case, this decision rests with the physician.

5. TIME FRAME FOR RECURRENT INTRODUCTION OF THE VIRAL VACCINES

A model of antitumor therapy with discontinuous trajectories of tumor growth (Equations (9)-(16)) was used to identify the time frame for recurrent viral vaccine introductions. The time length between the recurrent vaccine introductions ΔT is equal to the interval between the moment of initial introduction τ_1 and τ_2 – the moment when the tumor size $N(\tau_1) = N(\tau_2)$.

Kinetic curves of tumor growth after the viral vaccine is introduced on τ_1 =1 day, with dosages between $V_0^{\exp} = 0,015$ to $V_0 = 2,67 \cdot V_0^{\exp} = 0,04$, indicate that the time frame for subsequent introduction lies in the range of ΔT = 14,5 days to ΔT = 18,9 days depending on the dosage. Therefore, if the tumor size is small, it can be stabilized through recurrent introduction of these dosages within 14,5 – 18,9 days.

When the tumor is already big, its size can be stabilized while it is dominated by the fraction of the fast-proliferating cells ($t^* = 35$ days). If the vaccine is initially introduced on τ_1 =25 day, stabilizing regimen can be implemented through subsequent administration of dosages that produce two-stage immune response. Introduction of dosages in the range of $V_0^{\exp} = 0,015$ to $V_0 = 3 \cdot V_0^{\exp} = 0,045$ within the time frame of ΔT =30,5 can stabilize the tumor size on its pre-treatment level as of day 25. This allows to avoid surgical removal of the tumor.

6. PREDICTION OF THE FREQUENCY OF REPEATED VIRAL VACCINE ADMINISTRATION FOR THE CLINICAL SETTING

The model used in this study allows to calculate the time frame for recurrent viral vaccine introductions for experimental animals. In humans, these time intervals will be different. However, it is possible to calculate their approximate duration by applying allometric relationship (16) that describes the dependence of the metabolic processes in mammals on their body weight [32, 33]:

$$m = a \cdot \nu^b \tag{16}$$

where m is the mammal's body weight, ν is the speed of the mammal's metabolic processes, a and b are constant parameters.

Research indicates that body weight and lifespan also follow an allometric relationship for both humans and laboratory mice [32-34].

If we find the logarithm of equation (16), we obtain a linear equation that connects the average body weight of various mammals and humans with their average life span Tl (Figure 8):

$$\ln m = b \cdot \ln Tl + \ln a = b \cdot \ln Tl + c \tag{17}$$

Regression analysis allowed to define the value of regression coefficient b = 2,4981, which characterizes the slope of the regression line.

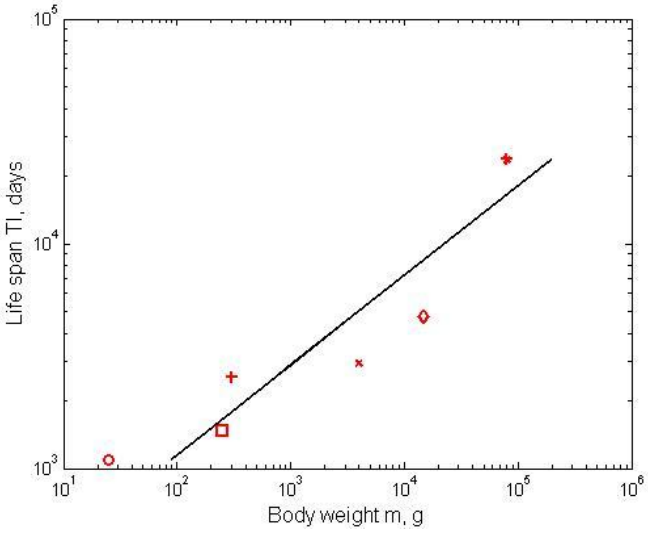

Figure 8. Dependence of the life span on body weight for ○ - mice, □ - rats, + - guinea pigs, x - rabbits, ◊ - dogs, and * - humans

Allometric relationships that define the tumor growth delay for mice and humans are as follows:

$$m^{human} = a \cdot \Delta T^{human}(V_0)^b \quad \text{and} \quad m^{mouse} = a \cdot \Delta T^{mouse}(V_0)^b \tag{18}$$

Where $\Delta T^{human}(V_0)$ is the duration of the tumor growth remission in a human after the viral vaccine administration in clinical oncology, $\Delta T^{mouse}(V_0)$ is duration of tumor growth delay in a mouse in the experiment.

The duration of tumor growth delay for a mouse and a human can be calculated using the following proportion

$$\frac{\Delta T^{human}(V_0)}{\Delta T^{mouse}(V_0)} = \left(\frac{m^{human}}{m^{mouse}} \right)^{\frac{1}{b}}$$

This proportion makes it possible to calculate the duration of tumor remission in humans based on the estimated tumor growth delay in mice (experimental group), average body weight of mice (experimental group), and human body weight:

$$\Delta T^{human}(V_0) = \Delta T^{mouse}(V_0) \cdot \left(\frac{m^{human}}{m^{mouse}} \right)^{\frac{1}{b}} \tag{19}$$

For the vaccine dosage $V_0 = V_0^{\max} = 0,024$ that produces the maximal number of antibodies against infected tumor cells, the periods between recurrent introductions for a mouse and a human will be as follows:

- For small tumors, when the vaccine is initially administered on τ_1 =1 day: $\Delta T^{mouse}(V_0)$ = 16,7 days**,** $\Delta T^{human}(V_0)$ =1,3 years;

- For bigger tumors, when the vaccine is initially administered on τ_1 =25 day: $\Delta T^{mouse}(V_0)$ = 30,5 days**,** $\Delta T^{human}(V_0)$ =2,1 years.

The period for the repeated vaccine introduction can be treated as a time when a patient needs to make a return visit to the therapist for examination. Examination will indicate whether the repeated administration of the vaccine is needed.

7. CONCLUSION

The software developed in MatLab-Simulink based on two mathematical models describing tumor growth after the introduction of antitumoral viral vaccines makes it possible to study the effectiveness of vaccine therapy for a wide range of dosages and times of introduction. The proposed algorithm for defining the optimal regimens of viral vaccine administration can be used for various types of experimental tumors and types of antitumor viral vaccines.

The results of the computing experiment presented in this paper make it possible to assess the effectiveness of different regimes of vaccine therapy. They suggest two strategies for the viral vaccine treatment. The first strategy allows a complete elimination of the tumor cells. This strategy implies a single-shot administration of a high dosage that produces the death of tumor cells at the 1st stage of immune response. The second strategy does not lead to the complete elimination of the tumor, but makes it possible to stabilize its size through recurrent introduction of the viral vaccine. If the initial tumor size is small, this stabilization gives the possibility to avoid the surgical intervention, with vaccine therapy acting as a regular vaccination against autologous tumor cells.

The present study also proposes the method of using experimental results to predict the duration of remission for the humans, based on allometric relationships. This method makes it

possible to define the time when a patient needs to make a return visit to the therapist for repeated examination and decision on whether further antitumor vaccine administration is required.

The development of high-tech methods for the treatment of oncological diseases is directly related to the cost of experimental research. Utilization of mathematical modeling at the different stages of experimental studies and on the stage of transferring the results to the clinical setting can reduce the cost of experiments and the length of research.

REFERENCES

[1] Dermime, S., Armstrong, A., Hawkins, R.E. & Stern, P.L. (2002) Cancer vaccines and immunotherapy. *British medical bulletin*, 62(1), 149-162.

[2] Mutsenietse, A. Ya. (1972) *Onkotropizm virusov i problema viroterapii zlokachestvennyh opuholej* [Oncotropism of viruses and the problem of viral therapy of malignant tumors]. Riga, USSR: Zinatne, [in Russian].

[3] Mutsenietse, A. Ya., Bumbieris, Ya. V., Bruvere, R. Zh. (1982) *Immunologija opuholej* [Immunology of tumors]. Riga, USSR: Zinatne, [in Russian].

[4] Moiseenko, V. M. (1999) Primenenie monoklonal'nyh antitel dlja lechenija zlokachestvennyh solidnyh opuholej [The use of monoclonal antibodies for the treatment of malignant solid tumors]. *Voprosy onkologii,* 45(4), 458-462, [in Russian].

[5] Gromova A. Yu. (1999) Protivoopuholevye svojstva vakcinnogo shtamma virusa venesujel'skogo jencefalomielita i ego onkolizata [Antitumor properties of the vaccine strain of the Venezuelan encephalomyelitis virus and its oncolyte]. *PhD Thesis (Biology),* St. Petersburg, [in Russian].

[6] Urazova, L. N. (2003) Jeffektivnost' i mehanizmy protivoopuholevogo dejstvija virusnyh vakcin pri jeksperimental'nom onkogeneze [Efficiency and mechanisms of the antitumor action of viral vaccines in experimental oncogenesis]. *PhD Thesis (Biology),* St. Petersburg, [in Russian].

[7] Vidyaeva I. G. (2005) Virusnye vakciny i ih onkolizaty v terapii jeksperimental'nyh opuholej [Viral vaccines and their oncolytes in the therapy of experimental tumors]. *PhD Thesis (Medicine),* Tomsk, [in Russian].

[8] Babushkina, N. A. (2005) Ispol'zovanie matematicheskogo modelirovanija dlja optimizacii rezhimov himioterapii na jeksperimental'nyh opuholjah [The use of mathematical modeling for the optimization of chemotherapy schedules on experimental tumors]. *Proceedings of the IV Int. Conf. SICPRO-05 "Identification of systems and control tasks"*, Moscow, [in Russian].

[9] Babushkina, N. A. (2011) Upravlenie processom himioterapii s ispol'zovaniem ferromagnitnyh nanochastic [Control of chemotherapy process with the use of ferromagnetic particles]. *Problemy upravlenija [Control sciences],* 3, 56-63, [in Russian].

[10] Babushkina, N. A. (2013) Ocenka upravljajushhih dozovyh vozdejstvij protivoopuholevoj vakcinoterapii s pomoshh'ju matematicheskogo modelirovanija [Evaluation of controlling dosage of vaccine therapy with the use of mathematical modeling]. *Problemy upravlenija [Control sciences],* 5, 60-65. [in Russian].

[11] Babushkina, N. A. & Glumov, V. M. (2014) Matematicheskoe modelirovanie mehanizmov protivoopuholevogo dejstvija virusnyh vakcin [Mathematical modeling of mechanisms of the antitumor action of viral vaccines]. *Proceedings of the IX Int. Conf. "Physics*

and radioelectronics in medicine and ecology" PHREME-2014. Vladimir, Russia, 1, 153-158, [in Russian]

[12] Babushkina, N. A. & Kuzina, E. A. (2015) Komp'juternye tehnologii na osnove matematicheskogo modelirovanija v sistemnoj jeksperimental'noj onkologii [Computer technologies based on mathematical modeling in the system of experimental oncology]. *Proceedings of the VIII Int. Conf. "Management of large-scale system development" (MLSD-2015).* Moscow, 272-284. [in Russian]

[13] Babushkina, N. A., Glumov, V. M. & Kuzina, E.A. (2016) Primenenie komp'juternyh tehnologij pri jeksperimental'nom izuchenii jeffektivnosti protivoopuholevyh virusnyh vakcin [The use of computer technology in the experimental study of the efficacy of antitumoral viral vaccines]. *Proceedings of the XII Int. Conf. "Physics and radioelectronics in medicine and ecology" PHREME-2016.* Vladimir, Russia, 1, 116-121. [in Russian]

[14] Babushkina, N. A., Glumov, V. M. & Kuzina, E. A. (2017) Primenenie matematicheskogo modelirovanija dlja ocenki jeffektivnosti metoda protivoopuholevoj terapii [Application of mathematical modeling for the evaluation of the effectiveness of the antitumor therapy method]. *Problemy upravlenija [Control sciences]*, 3, 49-56. [in Russian]

[15] Loktev, V.B., Ivankina T.Yu., Netesov S.V. & Chumakov P.M. (2012) Onkoliticheskie parvovirusy. Novye podhody k lecheniju rakovyh zabolevanij [Oncolytic parvoviruses. New approaches to the treatment of cancer diseases]. *Vestnik Rossijskoj akademii medicinskih nauk [Bulletin of the Russian Academy of Medical Sciences]*, 2, 42–47. [in Russian].

[16] Lezhnin Yu.N., Kravchenko Yu.E., Frolova E.I., Chumakov P.M., Chumakov S.P. (2015) Onkotoksicheskie belki v protivorakovoj terapii: Mehanizmy dejstvija [Oncotoxic proteins in anticancer therapy: Mechanisms of action]. *Molekuljarnaja biologija [Molecular Biology]*, 49(2), 264-278. [in Russian].

[17] Hristov G., Krämer, M., Li, J., El-Andaloussi, N., Mora, R., Daeffler, L., Zentgraf H., Rommelaere J., Marchini, A. (2010) Through its nonstructural protein NS1, parvovirus H-1 induces apoptosis via accumulation of reactive oxygen species. *Journal of virology*, 84(12), 5909-5922.

[18] Rommelaere J., Geletneky K., Angelova A.L., Daeffler L., Dinsart C., Kiprianova I., Schlehofer J.R., Raykov Z. (2010) Oncolytic parvoviruses as cancer therapeutics. *Cytokine & growth factor reviews,* 21(2), 185-195.

[19] Cotmore S. F. & Tattersall P. (2007) Parvoviral host range and cell entry mechanisms. *Advances in virus research*, 70, 183-232.

[20] Moehler M. H., Zeidler M., Wilsberg V., Cornelis J. J., Woelfel T., Rommelaere J., GalleP. R., Heike M. (2005) Parvovirus H-1-induced tumor cell death enhances human immune response in vitro via increased phagocytosis, maturation, and cross-presentation by dendritic cells. *Human gene therapy*, 16(8), 996-1005.

[21] Grekova S. P., Aprahamian M., Daeffler L., Leuchs B., Angelova A., Giese T., Galabov A., Helle rA., Giese N. A., Rommelaere J., Raykov Z. (2011) Interferon γ improves the vaccination potential of oncolytic parvovirus H-1PV for the treatment of peritoneal carcinomatosis in pancreatic cancer. *Cancer biology & therapy*, 12(10), 888–895.

[22] Raykov Z., Grekova S., Galabov A.S., Balboni G., Koch U., Aprahamian M., Rommelaere J. (2007) Combined oncolytic and vaccination activities of parvovirus H-1 in a metastatic tumor model. *Oncology reports*, 17(6), 1493-1500.

[23] Angelova A. L.,Aprahamian M., Balboni G.,Delecluse H. J., Feederle R., Kiprianova I., Grekova S., Galabov A., Witzens-Harig M., Ho A. D., Rommelaere, J., Raykov Z. (2009)

Oncolytic rat parvovirus H-1PV, a candidate for the treatment of human lymphoma: In vitro and in vivo studies. *Molecular Therapy*, 17(7), 1164–1172.

[24] Marchuk G.I. (1991) *Matematicheskie modeli v immunologii. Vychislitel'nye metody i jeksperimenty [Mathematical models in immunology. Computational methods and experiments]*. Moscow: Nauka, [in Russian]

[25] Romanyukha A.A. (2011) *Matematicheskie modeli v immunologii i jepidemiologii infekcionnyh zabolevanij [Mathematical models in immunology and epidemiology of infectious diseases]*. Moscow: BINOM. Laboratorija znanij, [in Russian]

[26] Bolodurina I.P., Lugovskova Yu.P. (2009) Optimal'noe upravlenie immunologicheskimi reakcijami organizma cheloveka [Optimum management of immunological responses of the human body]. *Problemy upravlenija [Control sciences]*, 5, 44–52, [in Russian]

[27] Rusakov S.V., Chirkov M.V. (2012) Matematicheskaja model' vlijanija immunoterapii na dinamiku immunnogo otveta [The mathematical model of the effect of immunotherapy on the immune response dynamics]. *Problemy upravlenija [Control sciences]*, 6, 45–50, [in Russian]

[28] Kogan, Y., Halevi–Tobias, K., Elishmereni, M., Vuk-Pavlović, S., & Agur, Z. (2012) Reconsidering the Paradigm of Cancer Immunotherapy by Computationally Aided Real-time Personalization. *Cancer Research*, 72(9), 2218 - 2227.

[29] de Pillis, L. G., Radunskaya, A. E., & Wiseman, C. L. (2005) A Validated Mathematical Model of Cell-Mediated Immune Response to Tumor Growth. *Cancer Research*, 65(17), 7950-7958.

[30] Palladini, A., Nicoletti, G., Pappalardo, F., Murgo, A., Grosso, V., Stivani, V., Ianzano, M.L., Antognoli, A., Croci, S., Landuzzi, L., De Giovanni, C., Nanni, P., Motta, S., Lollini, P.-L. (2010) In silico Modeling and In vivo Efficacy of Cancer-Preventive Vaccinations. *Cancer Research*, 70(20), 7755-7763.

[31] Skipper, H.E. (1971) Kinetics of mammary tumor cell growth and implications for therapy. *Cancer*, 28(6), 1479-1499.

[32] Monichev A.Y. (1984) *Dinamika krovetvorenija* [Dynamics of hematopoiesis]. Moscow: Medizina, [in Russian]

[33] Monichev, A. Y. (1987) A mathematical model of the spatial structure of bone marrow in hemopoietic dynamics. *Cybernetics and Systems Analysis*, 23(2), 274-280.

[34] Kuzina E.A., Babushkina N.A. (2016) Programmnaja realizacija metoda prognozirovanija jeffektivnosti vakcinoterapii ot jeksperimenta v kliniku [Software implementation of the method for predicting the efficacy of vaccine therapy from experiment to the clinic]. *Proceedings of the XII Int. Conf. "Physics and radioelectronics in medicine and ecology" PHREME-2016.* Vladimir, Russia, 1, 125-130, [in Russian]

APPENDIX 1. VALUES OF THE MODELS' PARAMETERS AFTER A SINGLE INTRODUCTION OF THE VIRAL VACCINE ON THE FIRST DAY OF THE TUMOR GROWTH

Equation	Parameter	Description
$\frac{dN(t)}{dt}$ – (9)	$\alpha_N = 3.3613$, $\beta_N = 0.0332$ $N_\infty = 23$ $N_0 = 0.75$	Parameters of the Gompertz function approximating the experimental growth curves of the tumor cell population without the vaccine administration (control sample)
$\frac{dN_V(t)}{dt}$ – (1)	$\tau_1 = 1$	Moment of the first introduction of the viral vaccine
	$Z_{CV} = 4.5$	Time lag of the immune response against the virus
	$Z_{CN} = 10.5$	Time lag of the immune response against the infected tumor cells
	$t_V = \tau_1 + Z_{CV}$	Starting moment of the immune response against the virus
	$t_N = \tau_1 + Z_{CN}$	Starting moment of the immune response against infected tumor cells
$\frac{dV(t)}{dt}$ – (3)	$\alpha_V = 0.1$	Rate of virus replication
	$\beta_V = 15$	Death rate of viruses due to their interaction with antibodies
	$V_0 = 0.015$	Dosage of the viral vaccine – the initial condition of equation (2)
$\frac{dA_V(t)}{dt}$ – (4)	$\alpha_A = 100$	Rate of antibodies' formation from a single plasma cell
	$\beta_{AV} = 70$	Rate of decrease in the number of antibodies due to interaction with viruses
	$\beta_A = 5$	Rate of decrease in the number of antibodies due to natural destruction
	$A_V^{\max} = 1.05$	Maximum calculated number of antibodies
$\frac{dC_V(t)}{dt}$ – (5)	$\alpha_C = 100$	Rate of antibodies' formation from a single plasma cell
	$\beta_{CV} = 4.5$	Dimension factor
	$C_{VN} = 0.001$	Initial number of plasma cells
$\frac{dA_N(t)}{dt}$ – (6)	$\alpha_{AN} = 30$	Rate of antibodies' formation from a single plasma cell
	$\beta_{AN} = 6.2$	Rate of decrease in the number of antibodies due to interaction with tumor cells
	$\beta_{NN} = 6.3$	Rate of decrease in the number of antibodies due to

		natural destruction
	A_N^{max} = 4.6445	Maximum calculated number of antibodies
$\frac{dC_N(t)}{dt}$ – (7)	α_{CN} = 76.677	Rate of formation of plasma cells
	β_{CN} = 38	Dimension factor
	C_{NN} = 0.0001	Initial number of plasma cells
$\frac{dN_V(t)}{dt}$ – (1)	K_V = 0.25 K_{AV} = 0.8 K_{AN} = 0.8	Constant coefficients of the dynamic equation for infected cells after a single introduction of the vaccine
$P(t)$ – (8)	α_p = 0.3 K_p = 0.95 β_p = 1/t*	Parameters of function P(t), describing the dynamic equation for reduction of the fast-proliferating fraction of tumor cells
	t*= 35 days	Moment when the number of fractions of rapidly proliferating cells is equal to the number of fractions of slowly proliferating cells
$\frac{dN(t)}{dt}$ –(10)	ε_V = 4.3 days	Length of the tumor cells' growth delay after their death at 1st stage of immune system stimulation
	ε_{CN} = 9.8 days	Length of the tumor cells' growth delay after their death at 2nd stage of immune system stimulation
	ε_{sum} = 14.1 days	Total length of the tumor cells' growth delay (1st and 2nd stage of immune system stimulation)
	t_1^V = 5.82 t_1^N = 12.32	Starting moments of the 1st and the 2nd stage of immune response
	t_2^V =7.13 t_2^N =14.288	Ending moments of the 1st and the 2nd stages of immune response
	$N_V^V(t_1^V)$ =1.3125 $N_V^N(t_1^N)$ =1.1458	Maximal numbers of infected tumor cells before the start of the 1st and the 2nd stages of immune response
	$N_V^V(t_2^V)$ = 0.84 $N_V^N(t_2^N)$ =0.1031	Minimal numbers of infected tumor cells before the end of the 1st and the 2nd stages of immune response
	$\Delta N_V^V(t_1^V)$ = 0.472, $\Delta N_V^N(t_1^N)$ = 1.043	Number of dead infected cells at the 1st and the 2nd stages of immune response

APPENDIX 2. KINETIC CURVES OF TUMOR GROWTH

Kinetic curves are calculated for varying dosages on two moments of introduction: τ_1 = day 1 (figures (a) – (b)) and τ_1 = day 25 (figures (c) – (d)).

For each dosage, figure (a) shows the dynamics of tumor growth $N(t)$ after viral vaccine administration (dotted line denotes the dynamics of the number of infected tumor cells $N_V(t)$), figure (b) shows the dynamics of the number of antibodies $A_V(t)$ against the virus (red line), and $A_N(t)$ against infected tumor cells (black line) at two stages of the immune response.

Dosage V_0 = ***0,015***

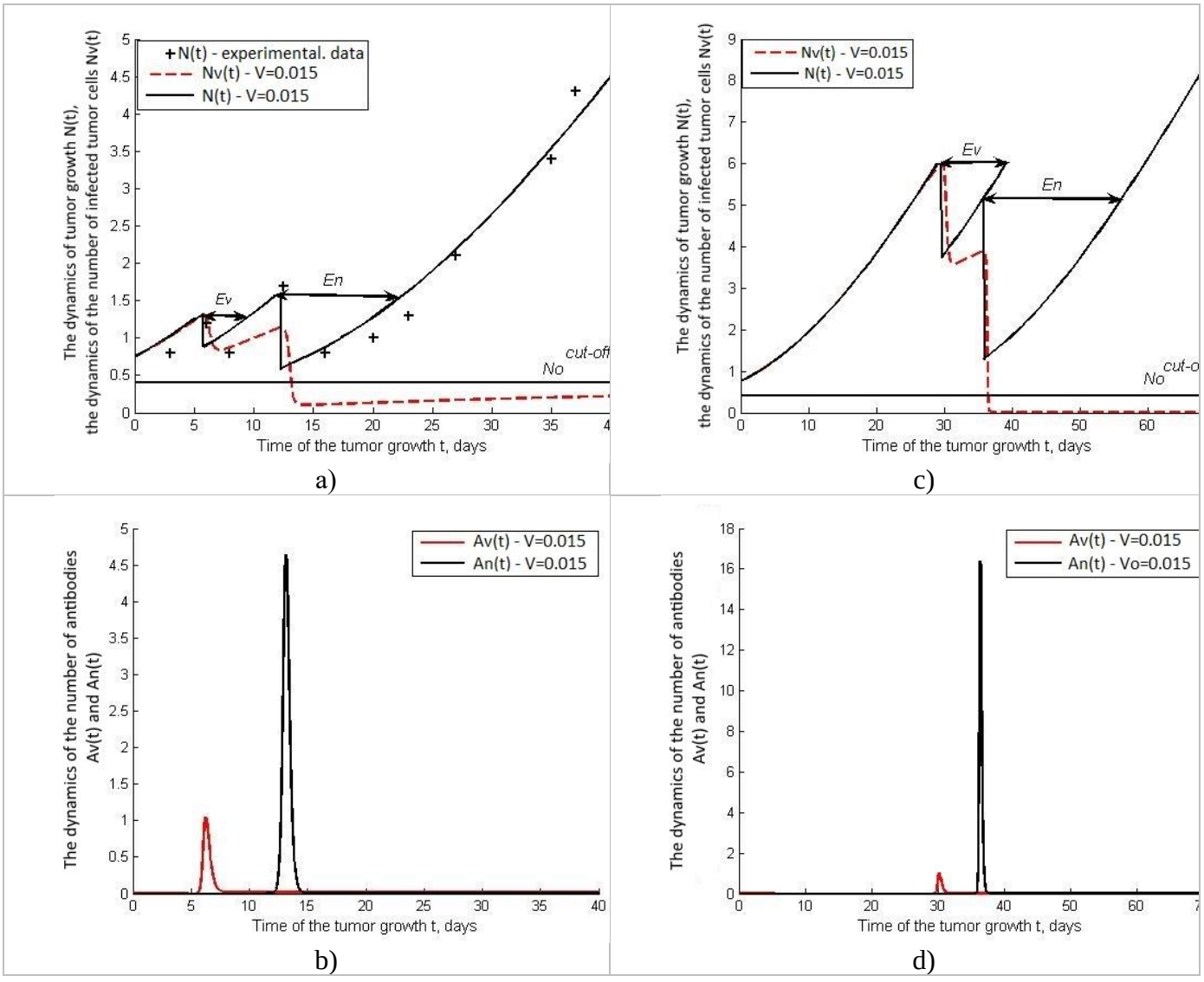

Dosage V_0 = ***0,024***

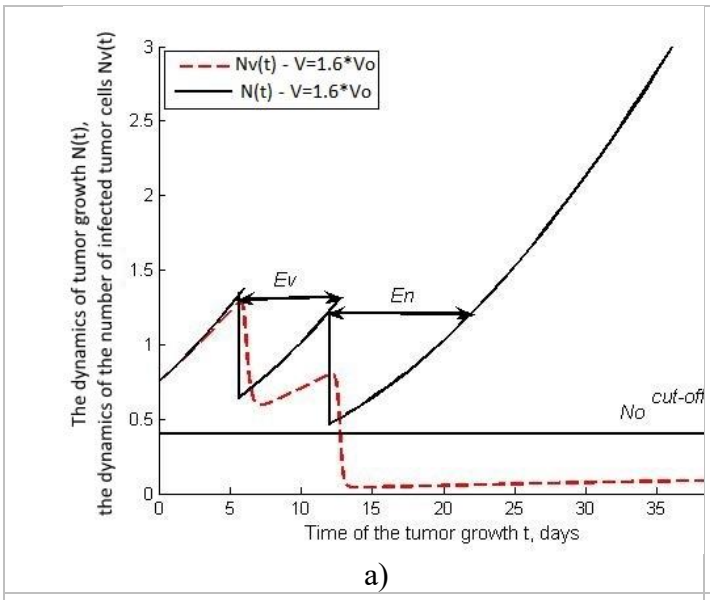

a)

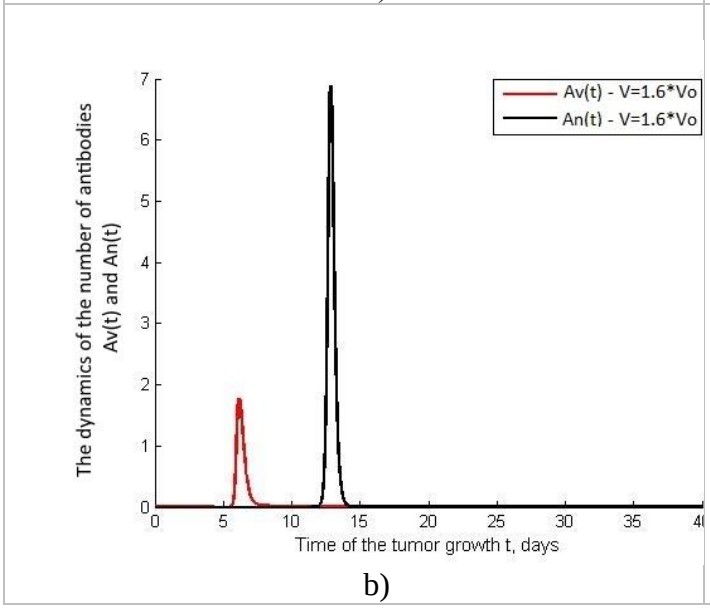

b)

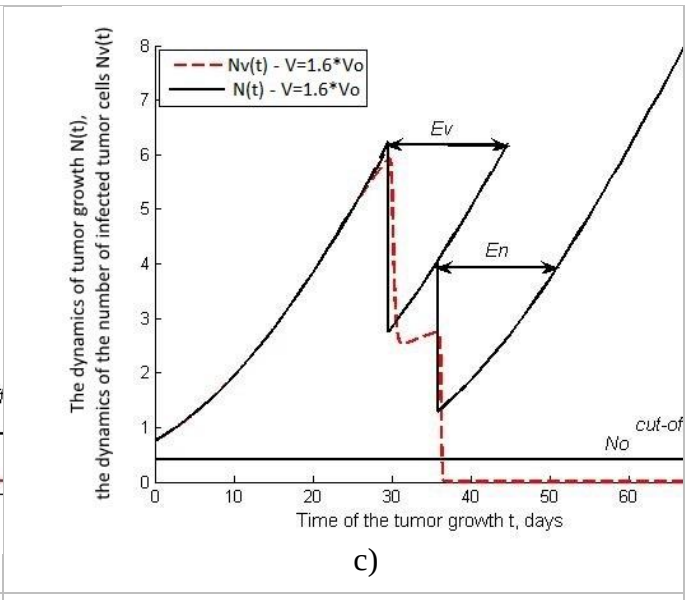

c)

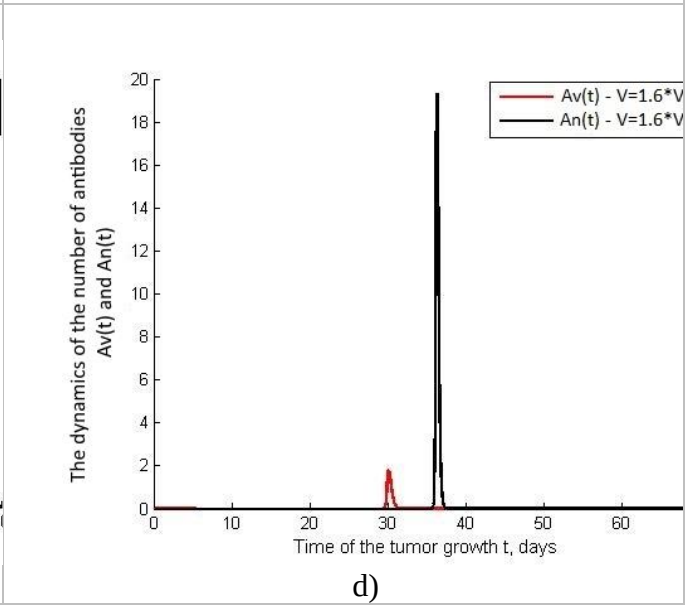

d)

Dosage V_0 = ***0,03***

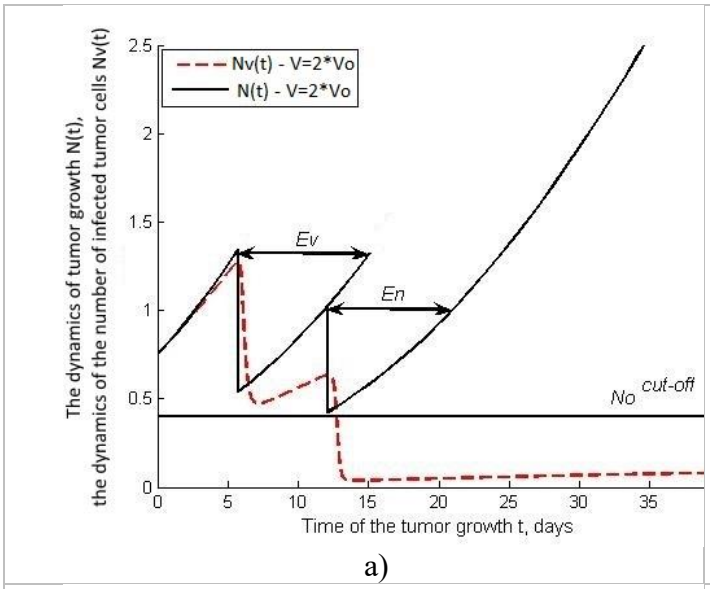

a)

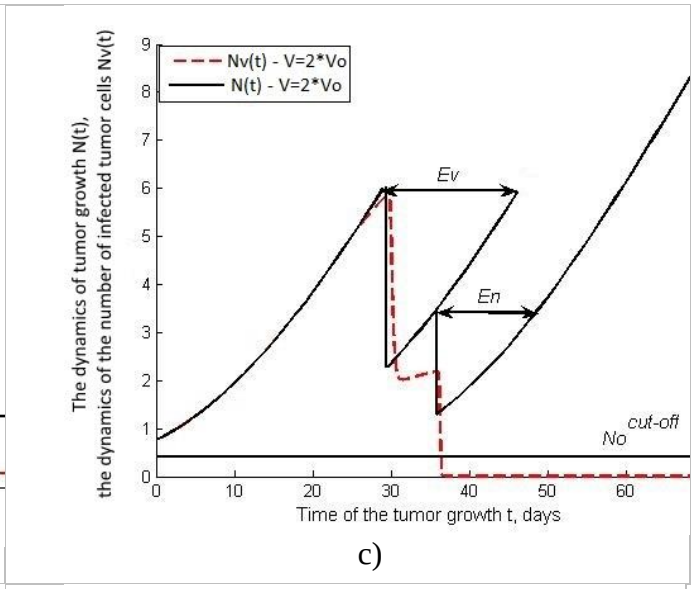

c)

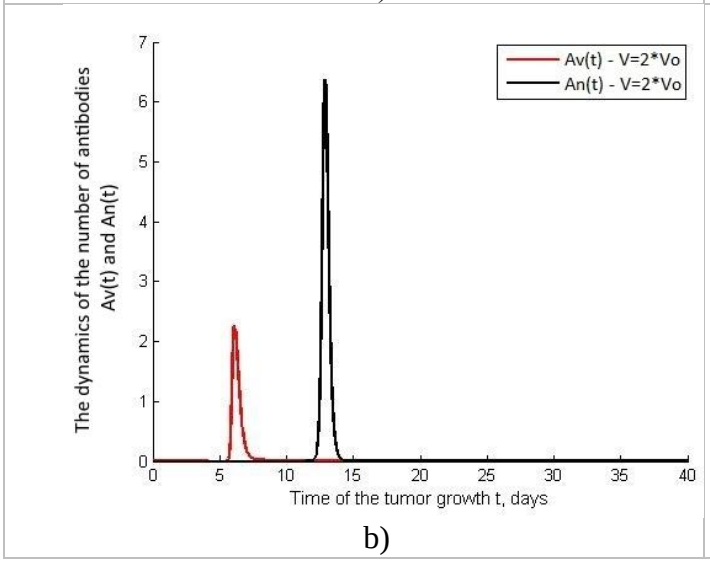

b)

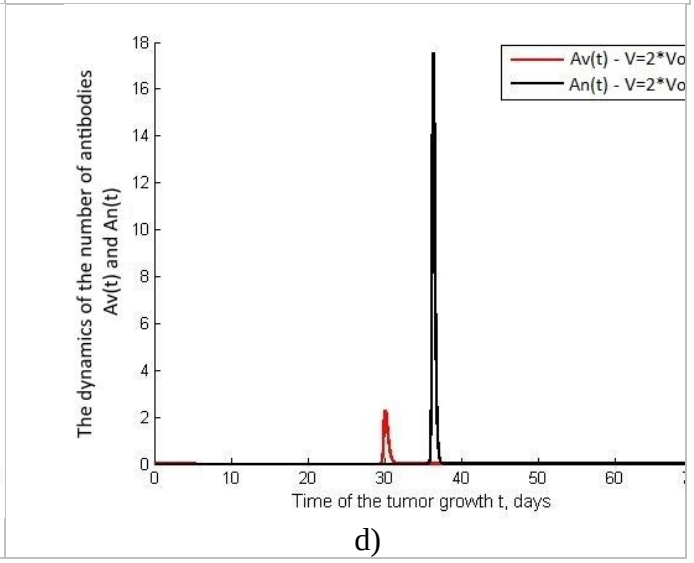

d)

Dosage V_0 = ***0,04***

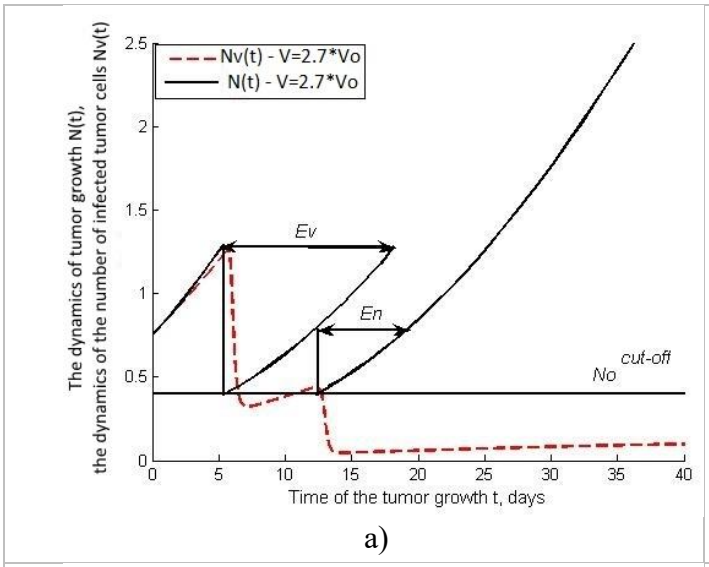

a)

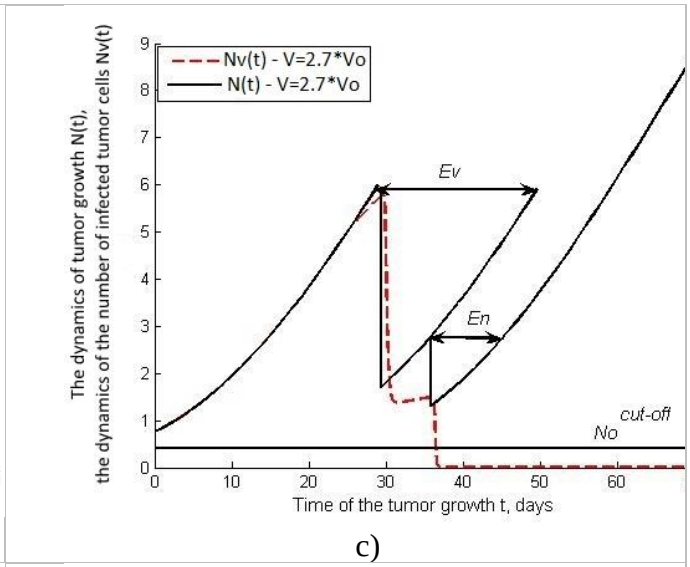

c)

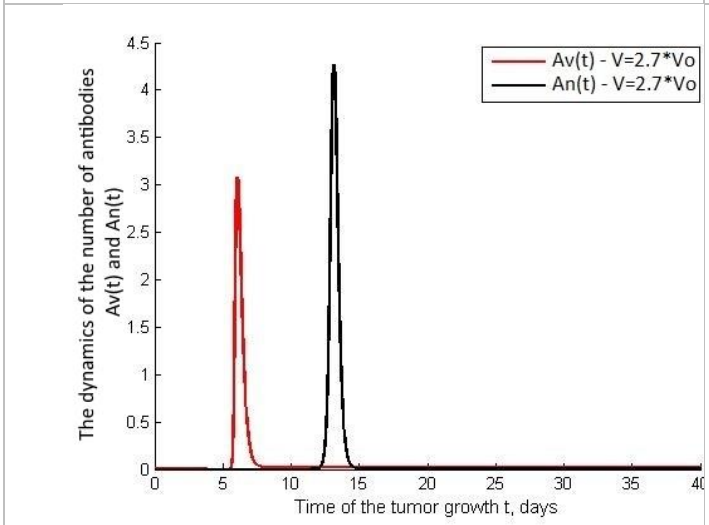

b)

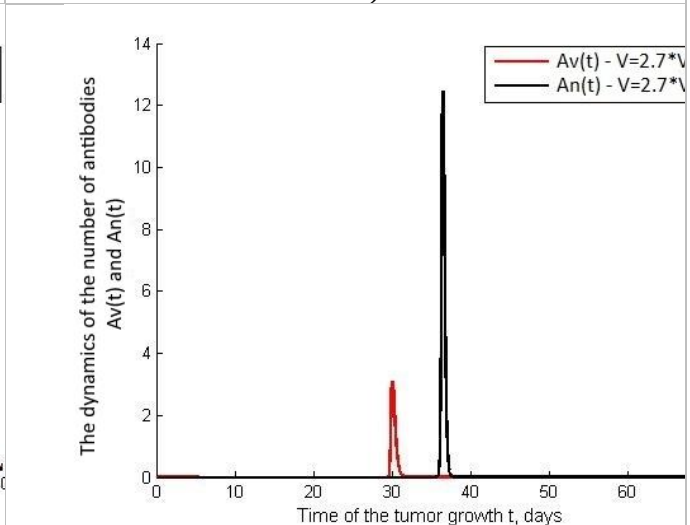

d)

Dosage V_0 = ***0,045***

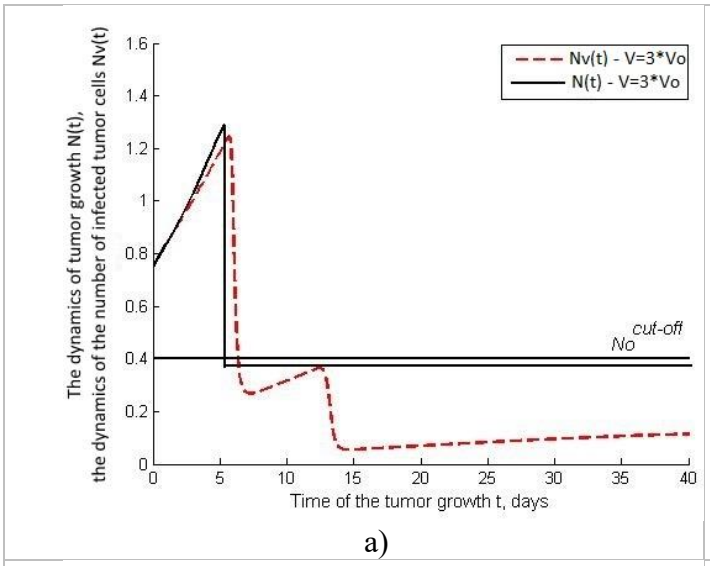

a)

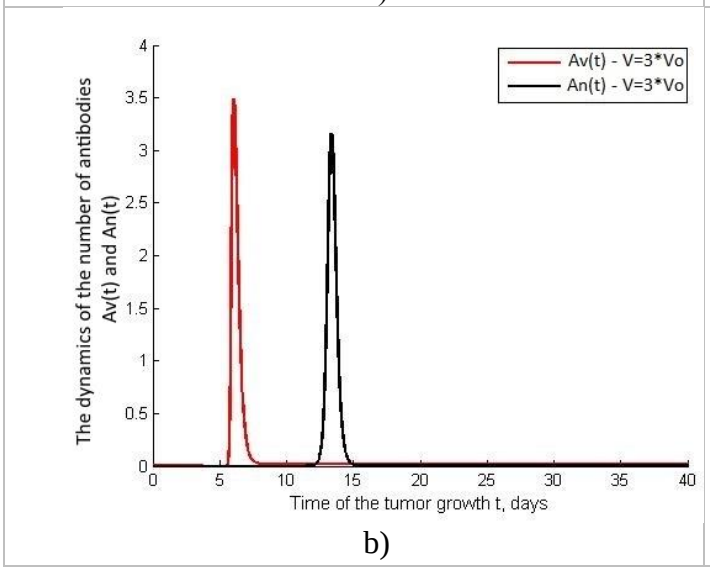

b)

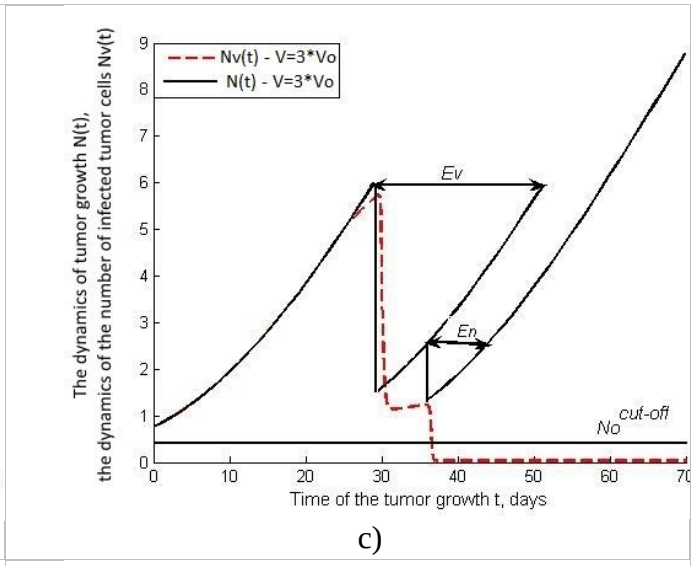

c)

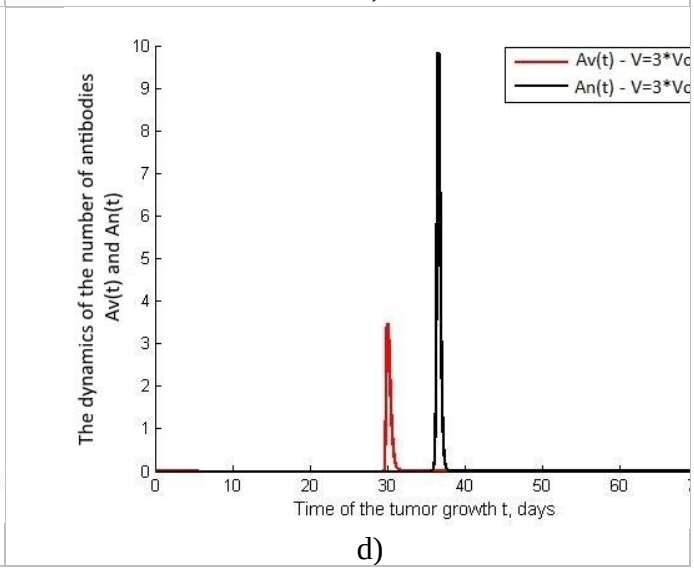

d)

Dosage V_0 = ***0,06***

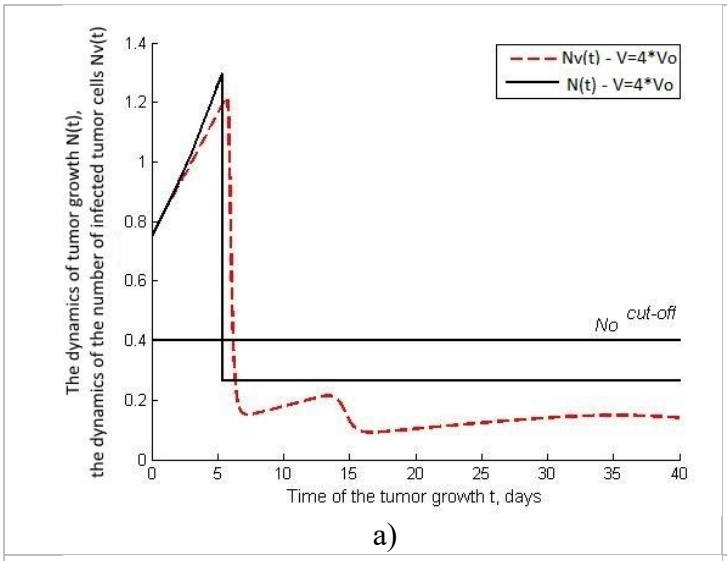

a)

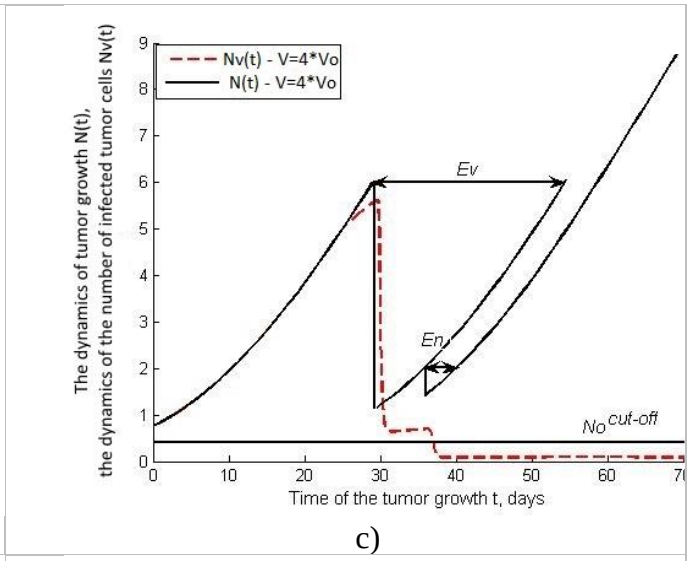

c)

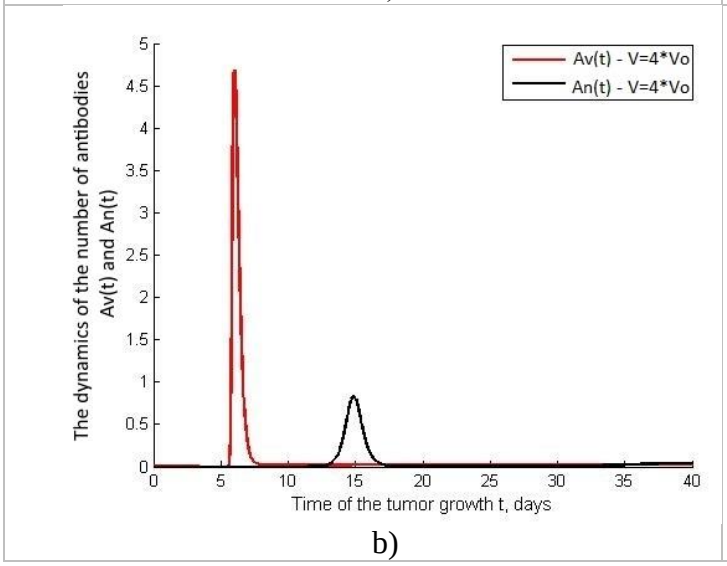

b)

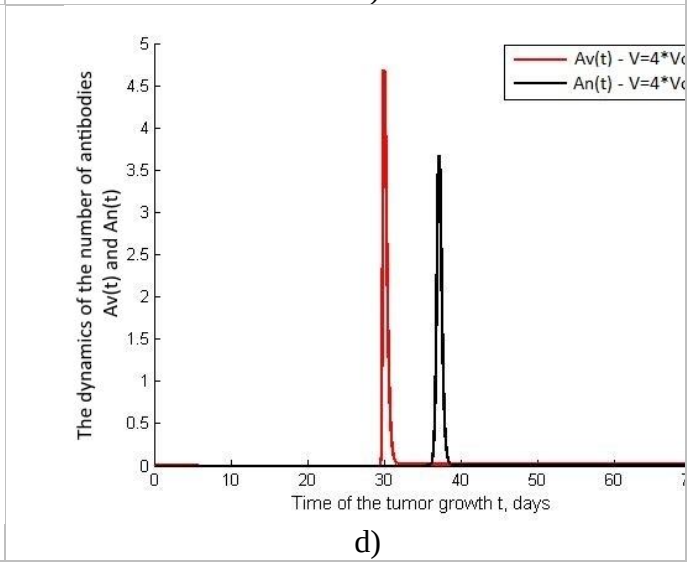

d)

Dosage V_0 = ***0,075***

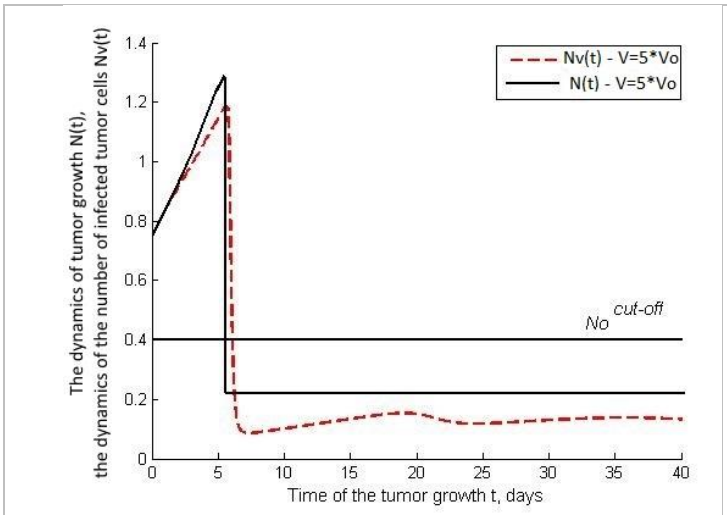

a)

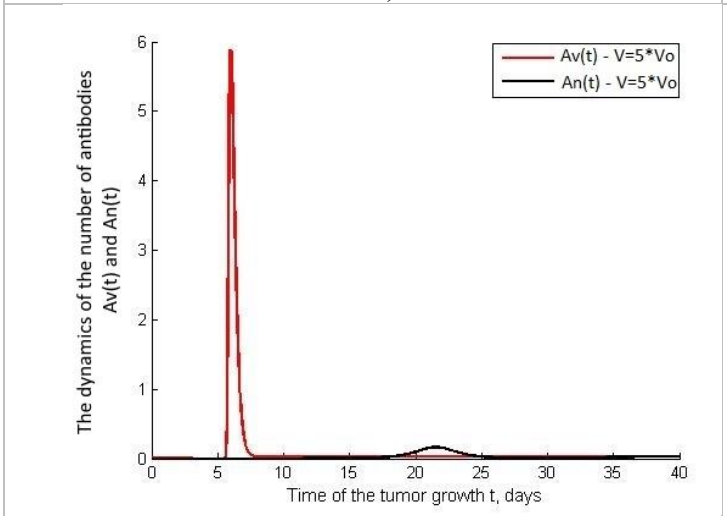

b)

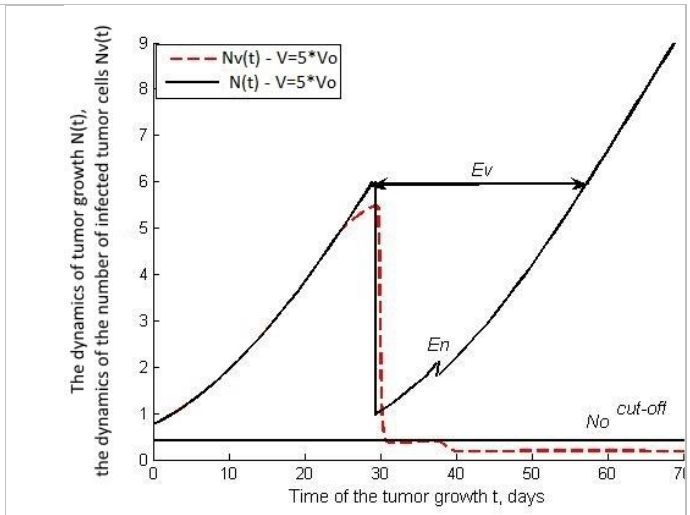

c)

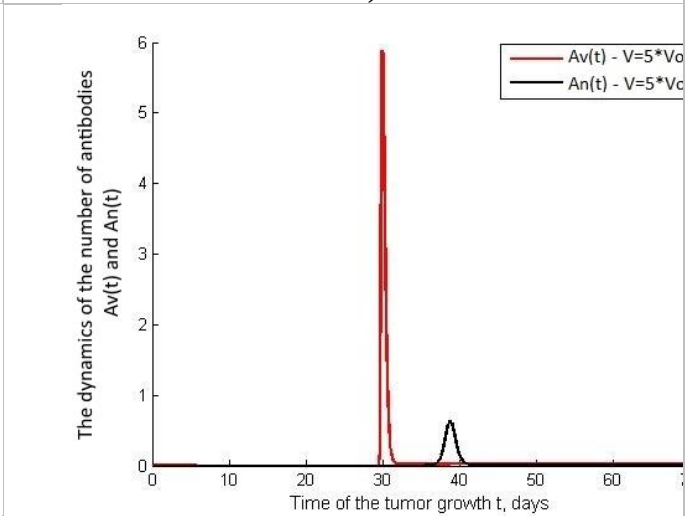

d)

Dosage V_0 = ***0,1***

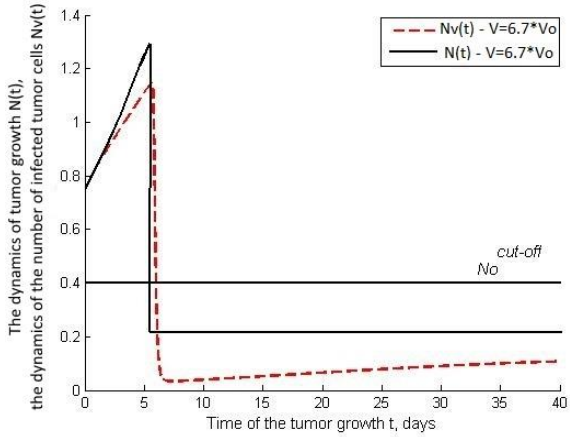

a)

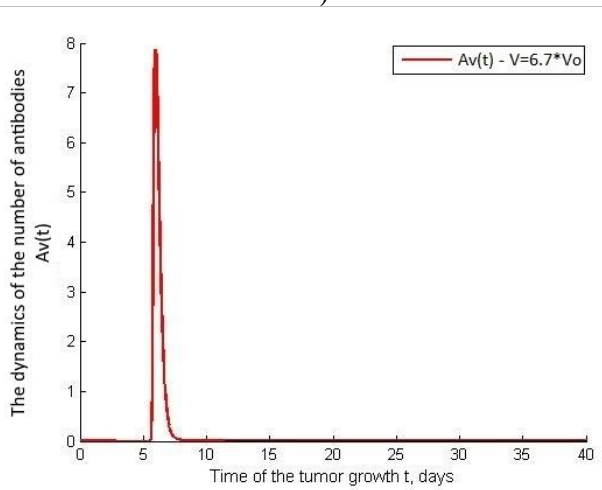

b)

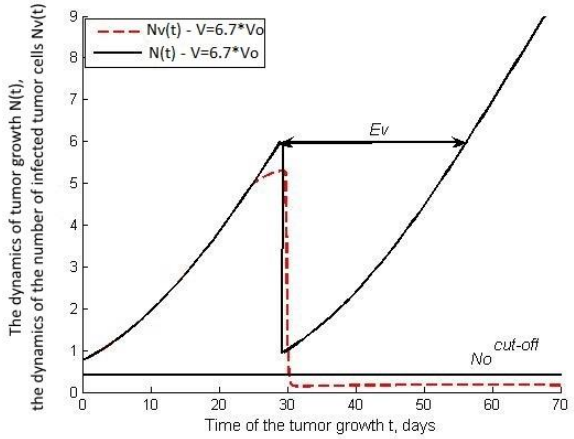

c)

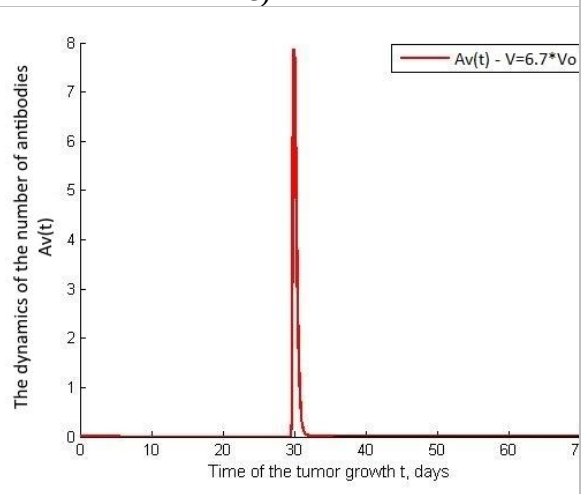

d)